



HAL
open science

Improved Isolation of SlaA and SlaB S-layer proteins in *Sulfolobus acidocaldarius*

Pierre Simonin, Carine Lombard, Arnaud Huguet, Adrienne Kish

► **To cite this version:**

Pierre Simonin, Carine Lombard, Arnaud Huguet, Adrienne Kish. Improved Isolation of SlaA and SlaB S-layer proteins in *Sulfolobus acidocaldarius*. *Extremophiles*, 2020, 24, pp.673-680. 10.1007/s00792-020-01179-9 . mnhn-02862458

HAL Id: mnhn-02862458

<https://mnhn.hal.science/mnhn-02862458>

Submitted on 17 Nov 2020

HAL is a multi-disciplinary open access archive for the deposit and dissemination of scientific research documents, whether they are published or not. The documents may come from teaching and research institutions in France or abroad, or from public or private research centers.

L'archive ouverte pluridisciplinaire **HAL**, est destinée au dépôt et à la diffusion de documents scientifiques de niveau recherche, publiés ou non, émanant des établissements d'enseignement et de recherche français ou étrangers, des laboratoires publics ou privés.

Title: Improved Isolation of SlaA and SlaB S-layer Proteins in *Sulfolobus acidocaldarius*

Authors and Affiliations: Pierre Simonin¹, Carine Lombard¹, Arnaud Huguet², and Adrienne Kish^{1*}

¹Muséum national d'Histoire naturelle, CNRS, Unité Molécules de Communication et Adaptation des Microorganismes UMR7245 MCAM, CP54, 57 rue Cuvier, 75005 Paris, France

²Sorbonne University, CNRS, EPHE, UMR 7619 METIS, 4, place Jussieu, Paris 75005, France

*Corresponding Author: Adrienne Kish, email: adrienne.kish@mnhn.fr

List of Abbreviations:

SDS = sodium dodecyl sulfate

SDS-PAGE = sodium dodecyl sulfate polyacrylamide gel electrophoresis

HEPES = 4-(2-hydroxyethyl)-1-piperazineethanesulfonic acid

EDTA = Ethylenediaminetetraacetic acid

MeOH = Methanol

DCM = Dichloromethane

HPLC-APCI-MS = high performance liquid chromatography-atmospheric pressure chemical ionization mass spectrometry

GDGT = glycerol dialkyl glycerol tetraethers

Pre-Print prior to peer review - see final version doi:10.1007/s00792-020-01179-9

1 **Abstract:**

2 The *Sulfolobus acidocaldarius* S-layer is composed of two main proteins: SlaA, which forms
3 the ordered structure of the S-layer matrix, and SlaB, which supports and anchors the S-layer
4 in the tetraether lipid membrane. Large batch-scale methods using starting culture volumes of
5 20-70 L have been developed for the isolation of the SlaA protein from the rest of the cell
6 envelope. These methods rely on the thermotolerance of SlaA and its high resistance to
7 detergents. SlaB, however, remains strongly associated in a large molecular weight aggregate
8 with other cell envelope components, even after removal of the remaining cellular contents.
9 Here we demonstrate a protocol for benchtop-scale (1-2 L) purification of S-layer proteins.
10 Using this protocol, we were also able to identify for the first time the tetraether lipids
11 strongly attached to SlaB.
12

13 **Keywords:** S-layer, cell wall, *Sulfolobus acidocaldarius*, Archaea, protein purification, SlaA,
14 SlaB
15

16 **Introduction:**

17 The cell walls of extremophilic microorganisms provides both vital protection from
18 potentially damaging agents, as well as an interface for interactions with both other
19 organisms and abiotic elements in the external environment. Cell wall composition varies
20 between different taxonomic groups, but most major phylogenetic groups of bacteria and
21 archaea include cell walls containing proteinaceous surface layers (or S-layers) (Zhu et al.
22 2017). S-layers can in fact be the sole component of the cell wall for many extremophilic
23 archaea.
24

25 S-layers are a self-assembling matrix of repeated protein monomers, often bearing post-
26 translational modifications such as glycosylations, that can modify the interactions between
27 cell surfaces and their surrounding biotic and abiotic environment. The symmetry of the S-
28 layer is determined by the number of monomers composing the repeated structural unit:
29 oblique (P2), square (P4), or hexagonal (P3 or P6). S-layer proteins are one of the most
30 abundant cellular proteins, composing in excess of 10 % of total protein (Sleytr et al. 2011).
31

32 S-layers are known to have roles in structural support, cell adhesion, and virulence
33 (Engelhardt 2007a). They have been shown to play key roles in the survival of extremophiles
34 under stress conditions, including salinity and osmotic stress (Engelhardt 2007b; Guan et al.
35 2012; Im et al. 2013), metal stress (Chandramohan et al. 2018), radionuclides (Merroun et al.
36 2005; Reitz et al. 2015), thermal stress and mechanical stress (Mader et al. 1999) as well as
37 enhancing UV resistance (Farci et al. 2017). S-layers have been harnessed for biotechnology
38 applications ranging from materials science, to metal biomining and bioremediation, to drug
39 delivery systems (Sleytr et al. 2011; Bartolomé et al. 2012; Sleytr et al. 2014; Ucisik et al.
40 2015).
41

42 S-layer proteins show little sequence conservation between the Bacteria and Archaea. Even
43 within the Archaea there is wide variance in the S-layer protein primary sequences and post-
44 translational modifications, as well as S-layer matrix symmetries, structures, and interactions
45 with the cell membrane and other cell envelope components (Albers and Meyer 2011;
46 Rodrigues-Oliveira et al. 2017). No complete crystal structure has been resolved to date for
47 archaeal S-layer proteins. The lack of conservation inhibits the development of "universal" S-
48 layer tools, such as universal S-layer recognition antibodies. Studies of S-layer proteins must
49 therefore be tailored to each taxonomic group, often employing model species.
50

51 The hyperthermoacidophilic *Sulfolobus acidocaldarius* has served as a key model for
52 studying the S-layers of archaea since its isolation in 1972 (Brock et al. 1972). Like other
53 *Sulfolobus* species, the S-layers of *S. acidocaldarius* are composed of monomers of the SlaA
54 protein self-assembled into a hexagonal array with threefold (P3) symmetry (Lembcke et al.
55 1991), and anchored into a tetraether monolayer cell membrane by the SlaB protein proteins
56 (Veith et al. 2009; Gambelli et al. 2019). Both SlaA and SlaB are known to be N-
57 glycosylated (Peyfoon et al. 2010; Guan et al. 2016). While *Sulfolobus* species share the same
58 the basic S-layer structure, the primary sequence of SlaA and SlaB share only 24-25 %
59 identify with other species such as *S. islandicus* and *S. solfataricus* {Gambelli:2019hd}. The
60 S-layer proteins of *S. acidocaldarius* also show far greater stability against detergents than
61 other *Sulfolobus* species. While *Sulfolobus solfataricus* and *Sulfolobus brierleyi* are only
62 mildly resistant to hot detergent (SDS) treatments, *S. acidocaldarius* was shown to be highly
63 resistant (König and Stetter 1986). Treatment with room temperature 10 % SDS resulted in S-
64 layer sheets, but the *S. acidocaldarius* S-layer proteins remained insoluble up to treatment
65 with 10 % SDS at 90 °C (Weiss 1974).

66
67 Many aspects of the S-layer structure and function can be studied using whole cells, however
68 isolation and purification of the S-layer proteins is needed to separate the roles of SlaA and
69 SlaB from those of the other cell envelope components. Despite the simplistic structure of the
70 *Sulfolobus* cell envelope, isolation of the S-layer proteins is complicated by the fact that after
71 an initial cell disruption and removal of the cellular contents, S-layer-containing cell-free
72 sacculi retain the same morphology as whole cells. These sacculi or "ghosts" can contain the
73 complete cell envelope (cell membrane, SlaA, SlaB); or only the cell wall (S-layer only, no
74 cell membrane).

75
76 Early extractions of the *S. acidocaldarius* cell envelope lysed cells using either a French
77 press, or detergents (0.15 % SDS with 10 mM EDTA) to aid in destabilizing the cell
78 envelope (Weiss 1974; Michel et al. 1980). Grogan (1989) developed a generalized
79 *Sulfolobus* S-layer purification protocol using 0.4 % N-lauryl sarcosine in buffer (pH 5) to
80 lyse cells and DNase treatment to reduce the lysate viscosity, followed by repeated cycles of
81 treatment with the same solution heated to 56 °C and centrifugation to remove cellular debris,
82 eventually producing a white upper phase containing the S-layer proteins overlaying the
83 brownish cell pellet. The higher resistance of *S. acidocaldarius* S-layer proteins to detergent
84 treatments compared to other *Sulfolobus* species were exploited to permitted better separation
85 of the S-layer proteins from the underlying cell membrane. Lipid removal was found to be
86 more effective using SDS rather than Triton X-100. Using large batches (over 20 L) of cell
87 cultures for extractions, it was found that following an initial cell lysis, repeated hot (60 °C)
88 SDS treatments could be employed to separate *S. acidocaldarius* S-layers from other cellular
89 proteins (Michel et al. 1980). SDS was subsequently removed by 6-8 washes in deionized
90 H₂O (dH₂O). This protocol became the standard for *S. acidocaldarius* S-layer extractions.

91
92 However, the composition of the protein extracts (SlaA, SlaB) varied between labs. Using the
93 same protocol and the same strain of *S. acidocaldarius*, one group reported obtaining S-layer
94 sacculi composed of both SlaA and SlaB proteins (Michel et al. 1980), while others reported
95 obtaining pure SlaA "ghosts" retaining cell-type morphology (Selenska-Pobel et al. 2011;
96 Reitz et al. 2015). The quantity of cell culture used for extraction also affects the quality of
97 the extracts. Following the same protocol, but using only 1 L of exponential-phase culture
98 instead of large batch cultures (20-70 L), we obtained S-layer ghosts with both SlaA and B
99 proteins rather than pure SlaA (Kish et al. 2016).

100

101 The inability to properly down-scaling the S-layer extraction protocol to benchtop scale (1-2
102 L) cultures, as well as the difficulties encountered isolating SlaB, likely due to the strong
103 association of SlaB with so-far unidentified molecules in the cell envelope, inhibit routine
104 studies of S-layer protein structure and function.

105

106 Here we present a method for a benchtop-scale purification of SlaA and SlaB proteins, as
107 well as characterization of the molecules strongly associated with the SlaB anchor protein.

108

109 **Methods and Results:**

110 The purification of SlaA and SlaB proteins followed three main steps: preparation of cell
111 envelope extracts, separation of SlaA and SlaB, and finally removal of membrane lipids from
112 SlaB.

113

114 Culture growth and preparation of S-layer-enriched cell envelope extracts

115 *Sulfolobus acidocaldarius* DSM 639 cells were cultivated in Brock's medium (Brock et al.
116 1972) pH 3.5 supplemented with 0.1% yeast extract and 0.2% D-saccharose at 80 °C with
117 agitation (170 rpm) in 1 L Erlenmeyer flasks with specialty-made extended glass aeration
118 necks in a shaking oil bath until mid-exponential growth phase ($OD_{600nm}=0.5$). The cells were
119 harvested by centrifugation (8000 x g, 10 min), and the cell pellets resulting from roughly 1 L
120 of culture were flash frozen in liquid nitrogen and stored at -80 °C until use for S-layer
121 protein extraction.

122

123 To purify the S-layer proteins, we first isolated the S-layer containing cell envelope using a
124 modified version of the protocol of Reitz et al. (Reitz et al. 2015), adapted to benchtop-scale
125 volumes (1-2 L cell culture at $OD_{600nm}=0.5$) rather than bioreactor-scale volumes (70 L) used
126 in previous studies. The cell pellet was gently thawed on ice and resuspended in HEPES
127 buffer (10 mM, pH 7) at 4 °C containing 2 mM EDTA to inhibit metalloproteases as well as
128 chelate any cations attached to anionic head of the tetraether membrane (Pineda De Castro
129 et al. 2016), and 1 mM Pefabloc SC to inhibit serine proteases (Fusi et al. 1991). Preliminary
130 disruption of cell membranes and solubilization of proteins was achieved using a denaturing,
131 anionic detergent (0.15 % SDS). DNA was digested by addition of 100 µg/µl DNase I and 4
132 mM MgCl₂ for 1 h at 37 °C to reduce the viscosity of the cell lysate. Further solubilization of
133 the cell lysate and cell membrane was then performed by overnight incubation in 2 % SDS at
134 room temperature with gentle agitation (50 rpm). Insoluble S-layer components were
135 separated from the rest of the solubilized cell lysate by centrifugation (40 000 x g, 45 min).
136 The white upper diffuse layer containing the cell envelope was removed from the more
137 compact, dark beige phase underneath, resuspended in the same buffer, and centrifuged as
138 before. The SDS was then removed from the resulting cell layer extracts by eight washes in
139 dH₂O (centrifugation at 40 000 x g, 45 min between each wash step), and the protein
140 components of extracts analyzed by SDS-PAGE.

141

142 This enriched S-layer protein sample obtained by hot SDS extraction was then analyzed by
143 SDS-PAGE. Solubilization of the proteins prior to electrophoretic migration was
144 accomplished by incubation in 20 mM sodium carbonate buffer (pH 10) at 65 °C for 30 min.
145 Laemmli buffer was then added and the proteins denatured at 95 °C for 5 min prior to
146 separation by SDS-PAGE (10 % gel), and visualized by Coomassie staining. The only two
147 bands visible (apparent masses near 120 kDa and 55 kDa) corresponded to the previously
148 established apparent molecular masses for polypeptides determined by mass spectrometry to
149 be SlaA and SlaB, respectively (Kish et al. 2016) (see Figure 1). More SlaA was isolated than
150 SlaB, which is coherent with the model for *Sulfolobus* S-layer structure, with six SlaA

151 proteins composing the hexameric S-layer array anchored by three SlaB proteins (Veith et al.
152 2009).

153

154 After removal of the supernatant, the resulting pellet contains two differently colored phases:
155 a lower, darker beige phase containing cell lysate and a whitish upper phase containing the
156 cell envelope. Previous protocols manually separated the whitish phase from the rest of the
157 pellet (Reitz et al. 2015). However, in practice obtaining a cell pellet sufficiently large to
158 easily manually separate the whitish phase from the darker phase is only possible when
159 starting from batch-scale culture volumes, such as the 70 L bioreactor used by Reitz et al.
160 (Reitz et al. 2015), which are not readily available. To separate the SlaA and SlaB proteins,
161 we instead used size exclusion chromatography.

162

163 Separation of SlaA and SlaB by size exclusion chromatography

164 The S-layer suspension in 20 mM Na-carbonate buffer (pH 10) was injected into a Superdex
165 200 (GE Healthcare) size exclusion chromatography column. Figure 2 shows the presence of
166 two peaks: the first is an exclusion peak (panel A; peak 1), whereas the second one
167 corresponds to purified SlaA monomers (panel A; peak 2). The purified SlaA monomers
168 were collected. In order to ensure that no SlaA monomers were mixed with SlaB proteins in
169 the excluded fraction, this fraction was reinjected and separated by gel filtration (Figure 2B;
170 peak 1'). The resulting fractions from both injections were stored at 4 °C. Separation of the
171 isolated proteins by SDS-PAGE (10 % gel; see Figure 3) revealed the expected apparent
172 molecular masses for purified SlaB and SlaA proteins in the first and second fractions,
173 respectively.

174

175 While this shows that the SlaA and SlaB proteins were successfully separated from all other
176 proteins, the chromatogram for the elution of the SlaB protein corresponds to a larger mass
177 than would be expected for SlaB monomers. We hypothesized that SlaB monomers were
178 aggregating, either due to hydrophobic interactions between SlaB proteins, or due to the
179 presence of membrane tetraether lipids still associated with the SlaB protein. To test the
180 hypothesis that lipids were remaining in association with SlaB even after treatment with 2%
181 SDS, we subjected the enriched SlaB fraction to lipid extraction.

182

183 Extraction and identification of membrane lipids associated with SlaB

184 The enriched SlaB suspension collected from the size exclusion chromatography column
185 (Figure 2B, peak 1') was dried using a rotary evaporator. Lipid extraction from the dried
186 sample was performed using a modified Bligh and Dyer method based on Huguet et al.
187 (2013). Briefly, samples were resuspended in an extraction mix of methanol
188 (MeOH):Dichloromethane (DCM):Buffer (either phosphate buffer (50 mM, pH 7.4) or Na-
189 carbonate buffer (40mM, pH 10)) (2:1:0.8 v/v/v), and placed in an ultrasonic bath (Branson
190 3510) for 10 min. The MeOH:DCM:Buffer (Phosphate or Na-carbonate) volume ratio was
191 then adjusted to 1:1:0.9, followed by centrifugation (500 x g, 10 min), and collection of the
192 extracts in a separation funnel. The DCM layer containing the lipids was separated from the
193 MeOH: Buffer (Phosphate or Na-carbonate) layer and then extracted three more times with
194 DCM, with the resulting DCM fractions combined and dried over Na₂SO₄. For extraction of
195 lipids from the enriched SlaB suspension, Na-carbonate (40 mM, pH 10) was used.

196

197 The lipid extract was then re-dissolved in 200 µL heptane and centrifuged using an
198 Eppendorf Mini Spin centrifuge (1 min, 7000 rpm). The supernatant was collected and
199 analyzed using high performance liquid chromatography–atmospheric pressure chemical
200 ionization mass spectrometry (HPLC–APCI–MS). Tetraether analyses were performed as

201 recently described by Huguet et al. (2019). Briefly, tetraether separation was achieved with
202 two silica columns in tandem (150 mm × 2.1 mm, 1.9 μm, Thermo Finnigan; USA)
203 thermostated at 40 °C. Injection volume was 30 μl. GDGTs were first eluted isocratically
204 with 82 % A/18 % B for 25 min (A = hexane, B = hexane/isopropanol 9/1, v/v). The
205 following linear gradient was subsequently used: 82 % A/18 % B to 65 % A/35 % B in 25
206 min, followed by 65 % A/35 % B to 100 % B, maintained for 10 min and then back to 82 %
207 A/18 % B in 10 min, maintained for 30 min. The flow rate was set at 0.2 ml/min.

209 HPLC-APCI-MS analysis enabled detection of two tetraether lipids in the sample of purified
210 SlaB proteins, identified on the chromatogram as two peaks with mass to charge ratios (m/z)
211 of 1296 at 10.7 min, and 1294 at 11.4 min (Figure 4A). These masses correspond to the
212 cyclopentane ring-bearing glycerol dialkyl glycerol tetraethers (GDGTs) GDGT-3 and
213 GDGT-4, respectively (Hopmans et al. 2000; Zeng et al. 2019).

215 To ensure that no other lipids remained attached to the SlaB proteins after lipid extraction,
216 the SlaB proteins obtained after solvent-based lipid extraction were first applied to a
217 Superdex 200 (GE Healthcare) size exclusion chromatography column. The resulting protein
218 fraction was then subjected to a second round of solvent-based lipid extraction using the
219 same protocol as previously, using phosphate buffer (50 mM, pH 7.4) instead of Na-
220 carbonate buffer, after which no lipids were detected (Figure 4B) with a minimum detection
221 limit of 1 ppb.

223 Having identified that GDGTs were in fact associated with SlaB after hot SDS treatment and
224 size exclusion chromatography, we sought to remove these lipids from the original SlaB
225 protein aggregate obtained after hot SDS treatment. This enriched SlaB protein solution
226 (Figure 2B, peak 1') was first solubilized in an equal volume of 20 mM Na-carbonate buffer
227 (pH 10) and then treated it with 1 % CHAPS for 30 min at 37 °C with agitation. To check
228 whether this treatment was sufficient for removal of the GDGTs associated with SlaB, the
229 CHAPS-treated solution was first applied to a Superdex 200 size exclusion chromatography
230 column to isolate the SlaB proteins which were excluded from the column, followed by lipid
231 extraction following the same modified Bligh and Dyer method described above using
232 phosphate buffer (50 mM, pH 7.4). HPLC-APCI-MS analyses failed to detect any
233 tetraether lipids in association with SlaB. The exclusion of SlaB proteins from the Superdex
234 200 resin indicates that despite the removal of residual GDGTs by CHAPS following hot
235 SDS isolation of the S-layer proteins, the SlaB proteins remained associated in an aggregate
236 mass.

238 Taken together, these results suggest that the larger mass observed during elution for purified
239 SlaB was due to both strong association with GDGTs and likely auto-aggregation of
240 hydrophobic, N-terminal transmembrane domain of the SlaB protein (Veith et al. 2009).

243 **Discussion :**

244 Here we present a method for complete isolation of SlaA from SlaB, starting from bench-
245 scale culture volumes. This method improves upon existing protocols by allowing for
246 reduced quantities of cell cultures to be used. In our study, the SlaA was found to have an
247 apparent molecular mass of 120 kDa, despite the calculated molecular mass of 151 kDa based
248 on its primary sequence (Claus et al. 2005). Previous studies have observed a range of
249 apparent molecular weights for SlaA from *S. acidocaldarius* DSM 639 up to 170 kDa
250 (Michel et al. 1980; Grogan 1989; Selenska-Pobel et al. 2011). Some early studies have even

251 shown two high-molecular weight bands for the SlaA protein (140 kDa and 170 kDa) that
252 were determined by their amino acid composition to be the same SlaA protein (Michel et al.
253 1980). This difference in the electrophoretic mobility of *S. acidocaldarius* S-layer proteins
254 has been attributed to protein glycosylations, as well as their low solubility in acidic or
255 neutral hot SDS (Grogan 1996). In addition, S-layer proteins remain insoluble in the neutral
256 pH Laemmli buffer containing SDS, and so prior to electrophoretic migration, S-layer
257 proteins must be solubilized in a heated alkaline buffer (Grogan 1989; Selenska-Pobel et
258 al. 2011; Guan et al. 2016). S-layer proteins from other archaea have shown altered
259 electrophoretic migration depending on culturing conditions including temperature, pH, and
260 protein maturation events (Konrad and Eichler 2002; Claus et al. 2005). While the reasons for
261 these differences in electrophoretic mobility are still unknown, attention must therefore be
262 paid when comparing results between studies using different strains of the same organism, as
263 well as the culturing and protein solubilization conditions.
264

265 This protocol allowed us to identify for the first time that the molecules aggregating with
266 SlaB in strong association are GDGTs. The interaction between SlaB S-layer anchor protein
267 and membrane tetraether lipids was shown to be highly resistant, even to heat and detergent
268 treatments. Less SlaB is present than SlaA, even in whole cells, coherent with the current
269 model for *Sulfolobus* S-layer structure with twice as much SlaA as SlaB (Veith et al. 2009).
270 There is likely some loss of SlaB during the initial steps of the extraction protocol due to
271 strong attachment to membrane lipids. The final SlaB extract contained no other proteins
272 detectable by SDS-PAGE or mass spectrometry, and no other lipids detectable using our
273 HPLC-MS methods. Despite this, the SlaB proteins still eluted from the size exclusion
274 chromatography column in the exclusion peak. This suggests that SlaB proteins strongly
275 associate with one another, likely due to interactions between monomers, likely due to
276 hydrophobic interactions between their N-terminal transmembrane domains.
277

278 Very little is currently known about the role of SlaB. The SlaB anchor protein of *S.*
279 *solfataricus* are predicted by its primary structure to be shorter than that of *S. acidocaldarius*,
280 containing fewer beta sandwich domains (Veith et al. 2009). Correspondingly, the pseudo-
281 periplasmic space created by the SlaB protein varies in height between the Sulfolobales, from
282 18 nm in *Sulfolobus shibatae* (Baumeister et al. 1989) to 27 nm in *S. acidocaldarius* (Kish et
283 al. 2016). A recent study of Δ *slaB* mutants in *Sulfolobus islandicus* suggests that the S-layer
284 anchoring role of SlaB can be partially complemented by another S-layer associated protein,
285 designated M164_1049 (Zhang et al. 2019). Another recent study in *Sulfolobus solfataricus*
286 used CRISPR-mediated silencing of gene encoding SlaB to show that in addition to its
287 anchoring role, SlaB is important in virus susceptibility, cell morphology, and cell division
288 (Zink et al. 2019).
289

290 These findings allow deeper study of the individual components of the essential cell envelope
291 structure. This is of particular importance given the current absence of tertiary structures for
292 archaeal S-layers, with the sole exception of the C-terminal domain of the *Methanosarcina*
293 *acetivorans* S-layer protein (Arbing et al. 2012). Extracted S-layers have been used in a range
294 of biotechnology applications, from nanomaterials and bioremediation applications, to
295 immobilized biocatalysts, biochips, and drug delivery (Selenska-Pobel et al. 2011; Bartolomé
296 et al. 2012; Sleytr et al. 2014). Historically, S-layer protein purity is often verified in relation
297 to other proteins by SDS-PAGE. Our results show the importance of analyzing for any
298 attached lipids to ensure protein purity prior to any sensitive downstream applications. Taken
299 together, the findings of this study will permit greater precision when isolating and studying

300 the S-layer components of Archaea, including their self-assembly, and interactions with other
301 macromolecules as well as ions and molecules in the extracellular environment.

302

303 **Acknowledgments.** This project was supported by grants to A. Kish from the CNRS MITI
304 program Xlife, and the MNHN (AVIV "Projet Fédérateur"). The authors wish to thank
305 Christelle Anquetil for help with HPLC-MS analysis of GDGTs.

306

307 **References:**

308 Albers S-V, Meyer BH (2011) The archaeal cell envelope. *Nat Rev Micro* 9:414–426. doi:
309 10.1038/nrmicro2576

310 Arbing MA, Chan S, Shin A, et al (2012) Structure of the surface layer of the methanogenic
311 archaean *Methanosarcina acetivorans*. *Proc Natl Acad Sci USA* 109:11812–11817. doi:
312 10.1073/pnas.1120595109

313 Bartolomé J, Bartolomé J, Bartolomé F, et al (2012) Strong paramagnetism of gold
314 nanoparticles deposited on a *Sulfolobus acidocaldarius* S layer. *Phys Rev Lett*
315 109:247203. doi: 10.1103/PhysRevLett.109.247203

316 Baumeister W, Wildhaber I, Phipps BM (1989) Principles of organization in eubacterial and
317 archaeobacterial surface proteins. *J Mol Biol* 35:215–227.

318 Brock TD, Brock KM, Belly RT, Weiss RL (1972) *Sulfolobus*: a new genus of sulfur-
319 oxidizing bacteria living at low pH and high temperature. *Arch Mikrobiol* 84:54–68.

320 Chandramohan A, Duprat E, Remusat L, et al (2018) Novel Mechanism for Surface Layer
321 Shedding and Regenerating in Bacteria Exposed to Metal-Contaminated Conditions.
322 *Front Microbiol* 9:3210. doi: 10.3389/fmicb.2018.03210

323 Claus H, Akça E, Debaerdemaeker T, et al (2005) Molecular organization of selected
324 prokaryotic S-layer proteins. *J Mol Biol* 357:731–743. doi: 10.1139/w05-093

325 Engelhardt H (2007a) Are S layers exoskeletons? The basic function of protein surface layers
326 revisited. *J Structural Biology* 160:115–124. doi: 10.1016/j.jsb.2007.08.003

327 Engelhardt H (2007b) Mechanism of osmoprotection by archaeal S-layers: a theoretical
328 study. *J Structural Biology* 160:190–199. doi: 10.1016/j.jsb.2007.08.004

329 Farci D, Slayov C, Piano D. 2017. Coexisting properties of thermostability and ultraviolet
330 radiation resistance in the main S-layer complex of *Deinococcus radiodurans*.
331 *Photochem Photobiol Sci* 17:1–8. doi: 10.1039/c7pp00240h

332 Fusi P, Villa M, Burlini N, et al (1991) Intracellular proteases from the extremely
333 thermophilic archaeobacterium *Sulfolobus solfataricus*. *Experientia* 47:1057–1060. doi:
334 10.1007/BF01923341

335 Gambelli L, Meyer BH, McLaren M, Sanders K, Quax TEF, Gold VAM, Albers S-V, Daum
336 B. 2019. Architecture and modular assembly of *Sulfolobus* S-layers revealed by electron
337 cryotomography. *Proc Natl Acad Sci USA* 8:1–9. doi: 10.1073/pnas.1911262116

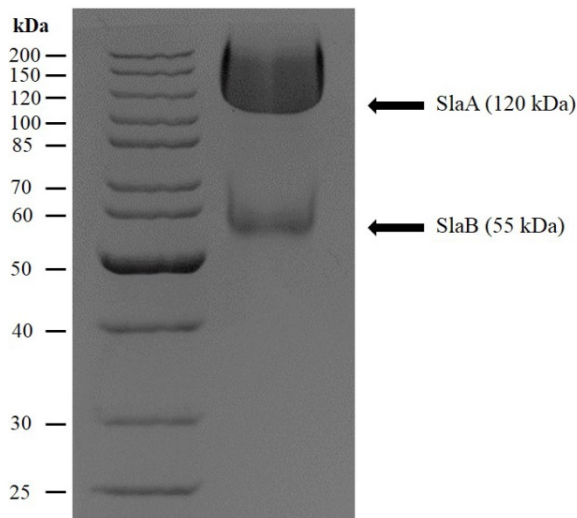
- 338 Grogan DW (1989) Phenotypic characterization of the archaeobacterial genus *Sulfolobus*:
339 comparison of five wild-type strains. *J Bacteriol* 171:6710–6719. doi:
340 10.1128/jb.171.12.6710-6719.1989
- 341 Grogan DW (1996) Organization and interactions of cell envelope proteins of the extreme
342 thermoacidophile *Sulfolobus acidocaldarius*. *Can J Microbiol* 42:1163–1171. doi:
343 10.1139/m96-148
- 344 Guan Z, Delago A, Nußbaum P, et al (2016) N-glycosylation in the thermoacidophilic
345 archaeon *Sulfolobus acidocaldarius* involves a short dolichol pyrophosphate carrier.
346 *FEBS Letters* 590:3168–3178. doi: 10.1002/1873-3468.12341
- 347 Guan Z, Naparstek S, Calo D, Eichler J (2012) Protein glycosylation as an adaptive response
348 in Archaea: growth at different salt concentrations leads to alterations in *Haloferax*
349 *volcanii* S-layer glycoprotein N-glycosylation. *Environmental Microbiology* 14:743–753.
350 doi: 10.1111/j.1462-2920.2011.02625.x
- 351 Hopmans EC, Schouten S, Pancost RD, et al (2000) Analysis of intact tetraether lipids in
352 archaeal cell material and sediments by high performance liquid
353 chromatography/atmospheric pressure chemical ionization mass spectrometry. *Rapid*
354 *Commun Mass Spectrom* 14:585–589. doi: 10.1002/(SICI)1097-
355 0231(20000415)14:7<585::AID-RCM913>3.0.CO;2-N
- 356 Huguet A, Coffinet S, Roussel A, et al (2019) Evaluation of 3-hydroxy fatty acids as a pH
357 and temperature proxy in soils from temperate and tropical altitudinal gradients. *Organic*
358 *Geochemistry* 129:1–13. doi: 10.1016/j.orggeochem.2019.01.002
- 359 Huguet A, Fosse C, Laggoun-Défarge F, et al (2013) Effects of a short-term experimental
360 microclimate warming on the abundance and distribution of branched GDGTs in a
361 French peatland. *Geochimica et Cosmochimica Acta* 105:294–315. doi:
362 10.1016/j.gca.2012.11.037
- 363 Im S, Joe M, Kim D, et al (2013) Transcriptome analysis of salt-stressed *Deinococcus*
364 *radiodurans* and characterization of salt-sensitive mutants. *Res Microbiol* 164:923–932.
365 doi: 10.1016/j.resmic.2013.07.005
- 366 Kish A, Miot J, Lombard C, et al (2016) Preservation of Archaeal Surface Layer Structure
367 During Mineralization. *Sci Rep* 6:26152–10. doi: 10.1038/srep26152
- 368 Konrad Z, Eichler J (2002) Lipid modification of proteins in Archaea: attachment of a
369 mevalonic acid-based lipid moiety to the surface-layer glycoprotein of *Haloferax*
370 *volcanii* follows protein translocation. *Biochem J* 366:959–964. doi:
371 10.1042/BJ20020757
- 372 König H, Stetter KO (1986) Studies on archaeobacterial S-layers. *Syst Appl Microbiol* 7:300–
373 309. doi: 10.1016/S0723-2020(86)80023-6
- 374 Lembcke G, Dürr R, Hegerl R, Baumeister W (1991) Image analysis and processing of an
375 imperfect two-dimensional crystal: the surface layer of the archaeobacterium *Sulfolobus*
376 *acidocaldarius* re-investigated. *J Microsc* 161:263–278. doi: 10.1111/j.1365-
377 2818.1991.tb03089.x

- 378 Mader C, Küpcü S, Sara M, Sleytr UB (1999) Stabilizing effect of an S-layer on liposomes
379 towards thermal or mechanical stress. *BBA Biomembranes* 1418:106–116.
- 380 Merroun ML, Raff J, Rossberg A, et al (2005) Complexation of uranium by cells and S-layer
381 sheets of *Bacillus sphaericus* JG-A12. *Appl Environ Microbiol* 71:5532–5543. doi:
382 10.1128/AEM.71.9.5532-5543.2005
- 383 Michel H, Neugebauer DC, Oesterhelt D (1980) The 2-D Crystalline Cell Wall of *Sulfolobus*
384 *acidocaldarius*: Structure, Solubilization, and Reassembly. In: *Electron Microscopy at*
385 *Molecular Dimensions*. Springer, Berlin, Heidelberg, Berlin, Heidelberg, pp 27–35
- 386 Peyfoon E, Meyer B, Hitchen PG, et al (2010) The S-layer glycoprotein of the crenarchaeote
387 *Sulfolobus acidocaldarius* is glycosylated at multiple sites with chitobiose-linked N-
388 glycans. *Archaea*. doi: 10.1155/2010/754101
- 389 Pineda De Castro LF, Dopson M, Friedman R (2016) Biological Membranes in Extreme
390 Conditions: Anionic Tetraether Lipid Membranes and Their Interactions with Sodium
391 and Potassium. *J Phys Chem B* 120:10628–10634. doi: 10.1021/acs.jpcc.6b06206
- 392 Reitz T, Rossberg A, Barkleit A, et al (2015) Spectroscopic study on uranyl carboxylate
393 complexes formed at the surface layer of *Sulfolobus acidocaldarius*. *Dalton Trans*
394 44:2684–2692. doi: 10.1039/c4dt02555e
- 395 Rodrigues-Oliveira T, Belmok A, Vasconcellos D, et al (2017) Archaeal S-Layers: Overview
396 and Current State of the Art. 8:2597. doi: 10.3389/fmicb.2017.02597
- 397 Selenska-Pobel S, Reitz T, Schöneman R, et al (2011) Magnetic Au nanoparticles on archaeal
398 S-Layer ghosts as templates. *Nanomaterials and Nanotechnology* 1:8–16.
- 399 Sleytr UB, Schuster B, Egelseer EM, et al (2011) Nanobiotechnology with S-layer proteins as
400 building blocks. *Prog Mol Biol Transl Sci* 103:277–352. doi: 10.1016/B978-0-12-
401 415906-8.00003-0
- 402 Sleytr UB, Schuster B, Egelseer EM, Pum D (2014) S-layers: principles and applications.
403 *FEMS Microbiol Rev* 38:823–864. doi: 10.1111/1574-6976.12063
- 404 Ucisik MH, Sleytr UB, Schuster B (2015) Emulsomes meet S-layer proteins: an emerging
405 targeted drug delivery system. *Curr Pharm Biotechnol* 16:392–405.
- 406 Veith A, Kingl A, Zolghadr B, et al (2009) *Acidianus*, *Sulfolobus* and *Metallosphaera*
407 surface layers: structure, composition and gene expression. *Mol Microbiol* 73:58–72. doi:
408 10.1111/j.1365-2958.2009.06746.x
- 409 Weiss RL (1974) Subunit cell wall of *Sulfolobus acidocaldarius*. *J Bacteriol* 118:275–284.
- 410 Zeng Z, Liu X-L, Farley KR, et al (2019) GDGT cyclization proteins identify the dominant
411 archaeal sources of tetraether lipids in the ocean. *Proc Natl Acad Sci USA*
412 12:201909306–7. doi: 10.1073/pnas.1909306116
- 413 Zhang C, Wipfler RL, Li Y, et al (2019) Cell Structure Changes in the Hyperthermophilic
414 Crenarchaeon *Sulfolobus islandicus* Lacking the S-Layer. doi: 10.1128/mBio.01589-19

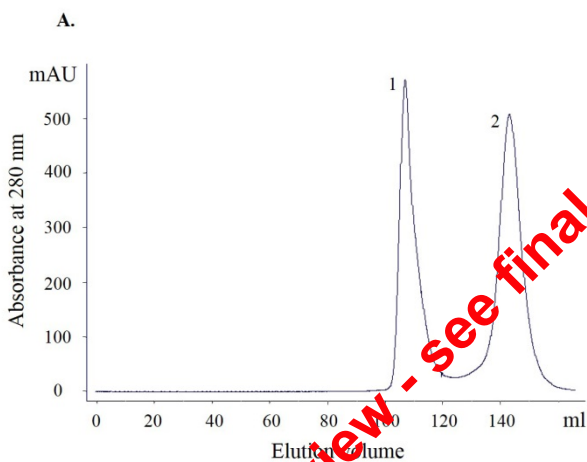
- 415 Zhu C, Guo G, Zhang F, et al (2017) Diversity in S-layers. Prog Biophys Mol Biol 123:1–15.
416 doi: 10.1016/j.pbiomolbio.2016.08.002
- 417 Zink IA, Pfeifer K, Wimmer E, et al (2019) CRISPR-mediated gene silencing reveals
418 involvement of the archaeal S-layer in cell division and virus infection. Nat Commun
419 10:4797–14. doi: 10.1038/s41467-019-12745-x

Pre-Print prior to peer review - see final version doi:10.1007/s00792-020-01179-9

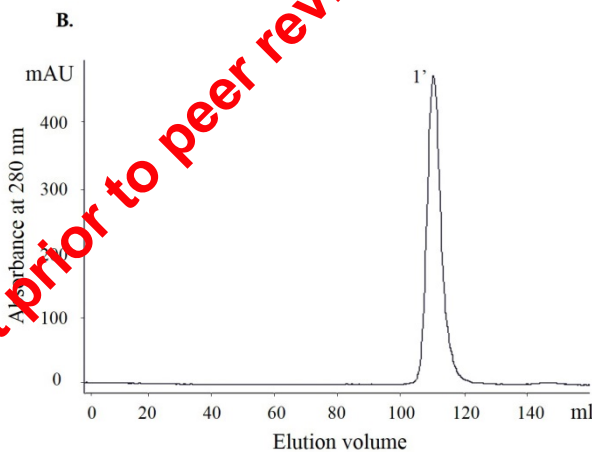
420 **Figures:**
421



422
423 Figure 1. SDS-PAGE of extracted S-layer ghosts with two bands with apparent molecular
424 masses around 120 kDa (SlaA) and 55 kDa (SlaB).
425
426

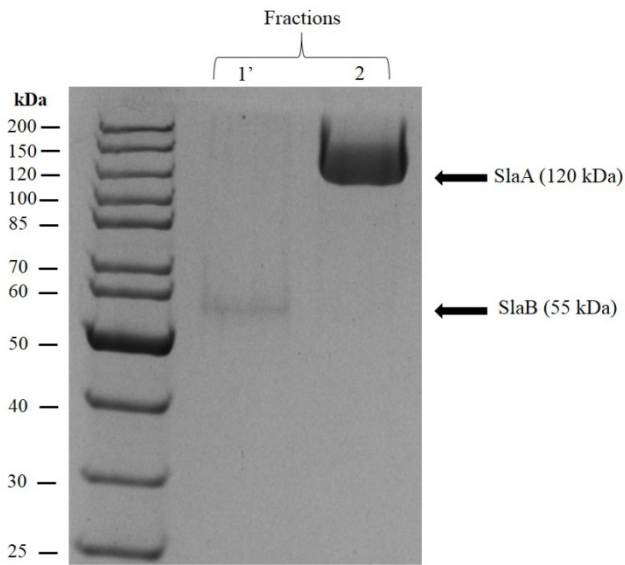


427



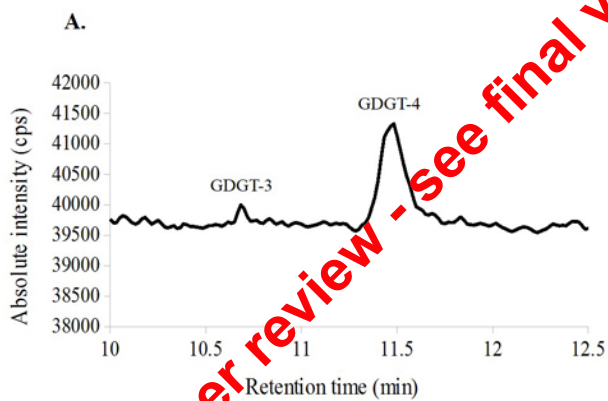
428
429 Figure 2. Separation of SlaA and SlaB protein by gel filtration chromatography. After
430 injection of the enriched S-layer protein sample obtained by hot SDS extraction (**panel A**) we
431 obtain two peaks; the peak 1 is an exclusion peak containing SlaB, whereas the peak 2
432 corresponds to purified SlaA monomers. To make sure that no SlaA monomers were mixed
433 with SlaB proteins in the excluded fraction, this fraction was then reinjected and separated by

434 gel filtration (**panel B**). The resulting exclusion peak exclusion (peak 1') shows that no
435 additional SlaA monomers were mixed in with the SlaB.
436

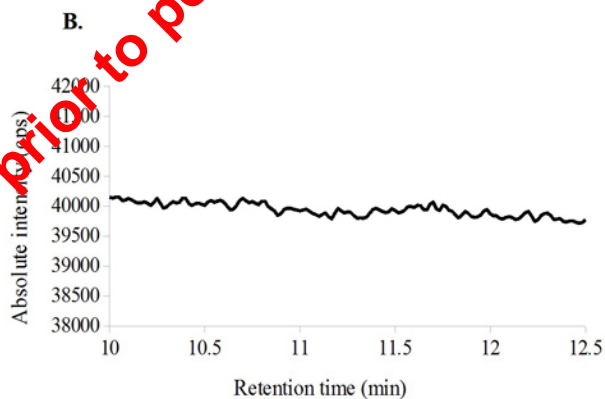


437
438 Figure 3. SDS-PAGE of fractions (1') and (2), resulting from the first and second injections
439 into the gel filtration column, respectively. The bands correspond to the expected apparent
440 molecular masses of SlaA and SlaB, showing that each protein extract is now free of other
441 polypeptides.

442
443



444



445

446 Figure 4. HPLC/MS identification of tetraether lipids present in samples of purified SlaB
447 before (**panel A**) and after (**panel B**) lipid extraction. The chromatograms show the absolute
448 intensity as a function of retention time.

Pre-Print prior to peer review - see final version doi:10.1007/s00792-020-01179-9